

UMFA: A photorealistic style transfer method based on U-Net and multi-layer feature aggregation

Dongyu Rao^a, Xiao-Jun Wu^{a,*}, Hui Li^a, Josef Kittler^b, Tianyang Xu^b

^aJiangnan University, Jiangsu Provincial Engineering Laboratory of Pattern Recognition and Computational Intelligence, School of Artificial Intelligence and Computer Science, Lihu Avenue, Wuxi, China, 214122

^bUniversity of Surrey, Centre for Vision, Speech and Signal Processing, Guildford, UK., GU2 7XH

1 **Abstract.** In this paper, we propose a photorealistic style transfer network to emphasize the natural effect of photo-
2 realistic image stylization. In general, distortion of the image content and lacking of details are two typical issues in
3 the style transfer field. To this end, we design a novel framework employing the U-Net structure to maintain the rich
4 spatial clues, with a multi-layer feature aggregation (MFA) method to simultaneously provide the details obtained by
5 the shallow layers in the stylization processing. In particular, an encoder based on the dense block and a decoder form
6 a symmetrical structure of U-Net are jointly staked to realize an effective feature extraction and image reconstruction.
7 Besides, a transfer module based on MFA and "adaptive instance normalization" (AdaIN) is inserted in the skip
8 connection positions to achieve the stylization. Accordingly, the stylized image possesses the texture of a real photo
9 and preserves rich content details without introducing any mask or post-processing steps. The experimental results
10 on public datasets demonstrate that our method achieves a more faithful structural similarity with a lower style loss,
11 reflecting the effectiveness and merit of our approach.

12 **Keywords:** photorealistic style transfer, U-Net, deep learning, AdaIN, Dense block.

13 *Xiao-Jun Wu, wu_xiaojun@jiangnan.edu.cn

14 1 Introduction

15 Photorealistic image stylization aims at realizing a style transfer between the two real photos. The
16 typical styles to be transferred include season,¹ weather and illumination *etc.*² It can be regarded
17 as a sub-problem of the wider class of style transfers. It differs from the general style transfer task
18 which employs realistic and artistic images to obtain artistic content images. The task of photore-
19 alistic style transfer is to achieve a realistic photo texture with natural stylized output. Therefore,
20 the photorealistic image stylization has a wide range of applications and excellent development
21 prospects in photo generation, picture processing, *etc.*

22 In the field of computer vision, style transfer is usually studied as a generalization problem
23 of texture synthesis,³ *i.e.*, extracting the texture from the source and transmitting it to the target.⁴

24 Traditional methods mainly focus on model building and texture synthesis.⁵ However, traditional

25 methods can only extract shallow features of the image without involving deep features, resulting
26 in the poor quality of the final appearance of the style transfer for complex images. Besides, the
27 constructed model is effective for a predefined specific style only.

28 With the emergence of deep learning, the use of deep features extracted by neural networks for
29 transforming a style has been widely developed.⁶⁻⁸ Gatys *et al.*⁶ proposed one of the first style
30 transfer methods based on deep convolutional neural networks.⁹ This method uses a convolutional
31 neural network to extract deep features and exploits the Gram matrix to characterize the style in
32 the image. By iteratively updating the reconstructed image, it realizes the stylization of the input
33 content image. This method can achieve a transfer of style effects even between complex images.
34 In addition, it solves the problem of applying a single model to different styles. This seminal work
35 has opened up a new field of research named Neural Style Transfer (NST).¹⁰ However, given a
36 new image, each process of the stylization model has to be retrained, increasing the computation.
37 Moreover, the tendency to distort the content image is notable. Subsequently, methods to improve
38 the quality of stylization and to accelerate the speed have been proposed.¹¹⁻¹⁴ Although these
39 methods achieve impressive artistic style transfer effects, they cannot suppress the distortion and
40 deformation of the content.

41 With the development of the neural style transfer field, in addition to the study of artistic style
42 transfer, other aspects of style transfer techniques are also of interest, such as style transfer of high-
43 resolution images, which is used to process HD images,^{15,16} text style transfer that changes text
44 attributes^{17,18} and photorealistic style transfer between real images.^{19,20}

45 Traditional methods of photorealistic style transfer are mainly based on color and tone match-
46 ing.²¹⁻²³ With the development of the neural style transfer, researchers have found that neural style
47 transfer could be used to realize the task of photorealistic image conversion. Based on the algo-

48 rithm proposed by Gatys, Fujun Luan *et al.*² were the first to tackle the photorealistic style transfer
49 task. Using the local affine transformation, inspired by the Matting Laplacian²⁴ in the color space
50 (RGB), the distortion of the content in the generated image is significantly reduced. Subsequently,
51 a series of algorithms, such as PhotoWCT,²⁵ WCT^{2, 20} and other methods^{19, 26} were proposed with
52 promising performance. They improved the quality of the generated images by changing the struc-
53 ture of the existing methods and introducing post-processing steps. However, the appearance of
54 stylized images produced by these methods is not natural. In addition, these methods introduce
55 more operating steps, increasing the processing time.

56 The key issue regarding the photorealistic image style transfer is how to keep the structure and
57 details of the content image while introducing the target style to achieve a natural stylized effect.
58 Meanwhile, there is one problem to be solved, *i.e.*, realizing the photorealistic style transfer in
59 real-time for the needs of real-world applications. Current methods cannot solve this problem very
60 well.

61 The specific objective of this study is to remove the distortion of the content in the stylized
62 image and to accelerate the natural stylization processing. In,^{20, 25, 27} the VGG network is used
63 to extract deep features to achieve image stylization. But these methods do not make full use of
64 the contextual information. In contrast, we propose to use dense block-based U-Net for feature
65 extraction and image reconstruction, retaining more image detail. Besides, feature aggregation is
66 an effective feature enhancement method in computer vision tasks. In order to tightly connect the
67 features, a multi-layer feature aggregation (MFA) method is proposed and used to enhance the
68 representation ability of the extracted features. In summary, we propose a new photorealistic style
69 transfer method named UMFA based on U-Net²⁸ and multi-layer feature aggregation.²⁹ The main
70 contributions of our method UMFA are as follows:

71 (1) A dense neural network architecture unit is used in a U-Net based style transfer framework.
72 The dense block enhances the quality of feature transferring. The benefit of the combination of
73 dense block and U-Net is the retention of spatial detail and the ability to express image content.

74 (2) A multi-layer feature aggregation method is used to fuse multi-scale features. The MFA
75 module strengthens the ability to express features, improving the stylization effect by introducing
76 aggregate features in each layer.

77 (3) The stylization process is carried out in the skip connection. Through a cascade processing
78 method, the directly stylized features are inserted into the image reconstruction process to achieve
79 a natural stylization effect.

80 The rest of our paper is structured as follows. In Section 2, we briefly review the photorealistic
81 style transfer method based on deep learning and the network structure used in this paper. In
82 Section 3, we present the proposed UMFA method in detail. In Section 4 we report, analyze, and
83 compare the experimental results. Finally, we summarize the main achievements and draw the
84 paper to the conclusion in Section 5.

85 **2 RELATED WORKS**

86 Recently, many researchers have adopted deep learning-based methods to realize photorealistic
87 style transfer between images and achieved very promising results.^{2,20,25} In this section, first, we
88 review several photorealistic image stylization methods based on convolutional neural networks.
89 Then we introduce the computational process known as the U-Net²⁸ structure. Finally, the problem
90 of feature aggregation is highlighted in the context of automatic style transfer and the main feature
91 aggregation mechanisms are discussed.²⁶

92 2.1 Deep Learning-based Photorealistic Style Transfer Methods

93 In 2016, Gatys et al. proposed the use of a VGG network³⁰ based method to extract features and
94 to perform art style image transfer. The authors deployed a pre-trained VGG model to obtain deep
95 features of the input image and a style image, and showed that a stylized image with both the target
96 content and the required style can be generated by optimizing a random noise image iteratively.
97 At the same time, their method of expressing style information with Gram matrix has also been
98 widely used. The Gram matrix is composed of the inner product of the two vectors, so the Gram
99 matrix can reflect the internal relationship between the vectors in the group of vectors. The deep
100 feature of an image can represent the structure, texture and other information of the image, so when
101 the Gram of the deep features of two images are similar, they have similar internal connections,
102 that is, they have similar styles.

103 Subsequently, Johnson et al.³¹ proposed an image style transfer method that uses a perceptual
104 loss to iteratively generate an optimized model named rapid style transfer. It greatly improves the
105 speed of the algorithm, but the model can work only for one style.

106 In 2017, Huang et al.²⁷ proposed an adaptive instance normalization (AdaIN) method inspired
107 by the notion of instance normalization (IN)^{32,33} for transferring arbitrary image styles. From a
108 statistical point of view, the style information of an image is also a kind of statistical information.
109 When two images have the same distribution, they also have similar styles. The "adaptive instance
110 normalization" is a method which changes the mean value and variance of the content image
111 feature and keeps it consistent with the mean value and variance of the style image to realize style
112 transfer.

113 Li et al.³⁴ developed a whitening and color transform (WCT) method for style transfer based

114 on a feature transform. These methods can achieve a real-time, arbitrary style transfer.

115 In 2018, Li et al.²⁵ proposed a technique called PhotoWCT, which further improves the base-
116 line established in.³⁴ This method changes the upsampling step to the unpooling operation in the
117 decoder, to smooth the final result. This method maintains the spatial consistency of the content
118 image and the stylized image. In 2019, Yoo et al.²⁰ proposed WCT² method inspired by WCT. This
119 method uses wavelet pooling instead of maximum pooling in.²⁵ Wavelet pooling retains the image
120 details, while the model introduces richer style elements through multi-level stylization operations.

121 The wide application of deep learning makes the design of the neural network structure an im-
122 portant factor affecting the model performance. Neural architecture search (NAS)³⁵ is a technol-
123 ogy for automatically designing efficient neural network structures. In 2020, An et al.²⁶ designed
124 a model for ultrafast photorealistic style transfer through neural architecture search. The basic
125 structure of this method is similar to WCT².²⁰ They searched for a neural architecture performing
126 a multi-layer stylization to optimise speed and convergence.

127 In addition to stylization methods based on the encoder and decoder networks, generative ad-
128 versarial networks (GAN) are also a hot research topic. Owing to their characteristics, the images
129 generated by a GAN tend to have realistic photo textures and natural appearance. Some methods ,
130 e.g. Pix2Pix,³⁶ AutoGAN³⁷ and others^{38,39} have reported remarkably good style transfer results.

131 2.2 *The U-Net Architecture*

132 In 2015, Ronneberger et al.²⁸ proposed a network structure for medical image segmentation named
133 U-Net. The structure consists of two main parts: encoder and decoder. The encoder includes con-
134 volutional layers and a pooling layer, which is constituted by a downsampling module. The de-
135 coder is a corresponding upsampling module. A skip connection between the corresponding layers

136 is added to retain rich detailed image information. In addition to medical image segmentation,
137 U-Net has achieved good results in semantic segmentation, image restoration, and enhancement.⁴⁰
138 Thanks to the U-Net structure, the image context is preserved and effectively used to reconstruct
139 the input image.

140 *2.3 The Feature Aggregation*

141 With the emergence of deep learning, deep features play an important role in computer vision
142 tasks. In order to improve the performance, the architecture of deep neural networks is increasingly
143 deeper and wider^{41,42} to enhance the modeling capacity and flexibility. Besides, tightening connec-
144 tions between layers is also an important factor affecting the performance of deep neural networks,
145 as proved by the idea of skip connection.⁴³ Feature aggregation can closely connect features of
146 different scales and levels to achieve a better quality of image reconstruction, as demonstrated in.²⁹

147 Inspired by these works, we adopt the U-Net structure for the task of style transfer and enhance
148 its modeling capability by endowing it with a multi-layer feature aggregation mechanism. Finally,
149 the merits of the proposed UMFA method based on U-Net and multi-layer feature aggregation are
150 demonstrated by extensive experiments.

151 **3 PROPOSED PHOTOREALISTIC STYLE TRANSFER METHOD**

152 In this section, we introduce the proposed UMFA method. First, we present the UMFA framework
153 in Section 3.1. The details of its training are presented in Section 3.2.

154 *3.1 UMFA: Photorealistic Style Transfer Network*

155 As shown in Fig. 1, UMFA consists of three main parts: encoder, decoder, and a transfer module.
156 The encoder and decoder constitute the basic symmetric structure of U-Net. The encoder includes

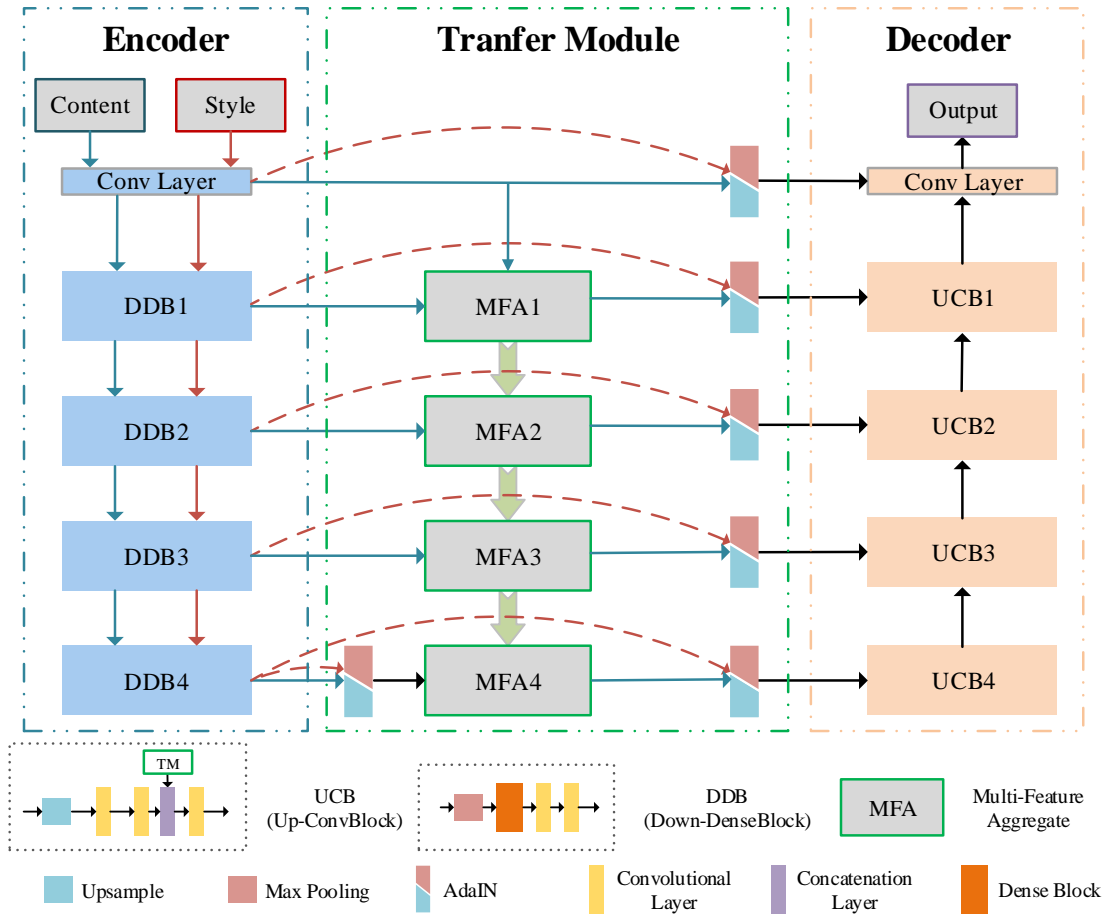


Fig 1 The framework of our method.

157 DDB blocks and a Conv Layer block. The decoder includes UCB blocks and a Conv Layer block.
 158 The remaining part of the architecture is the "transfer module" which includes MFA blocks and
 159 AdaIN blocks. In the encoder, the red and blue solid lines represent the features of the style image
 160 and content image, respectively.

161 In the "transfer module", blue solid line represents the characteristics of the content image. To
 162 make it easier to distinguish in the figure, the red dashed line is used to represent the characteristics
 163 of the style image. The black lines indicate stylized features. The features of the style and con-
 164 tent images are extracted by the encoder as a prerequisite to a style transfer through the "transfer
 165 module". The decoder reconstructs the output image.

166 In Fig. 1, "Conv Layer" represents convolutional layer. "DDB" means downsampling dense
167 block⁴⁴ which contains a max-pooling layer, a dense block, and two convolutional layers. The
168 framework of dense block is shown in Fig. 2 (b). Three convolutional layers are densely connected
169 to form a dense block. "UCB" denotes upsampling convolutional block which has an upsampling
170 layer, three convolutional layers and a concatenation module that connects information coming
171 from the "transfer module". "MFA" represents multi-layer feature aggregation at skip connection.
172 In Fig.2 (a), the structure of "MFA" is displayed, where "Concat Layer" represents the cascade
173 of the features passed from the previous with the features of layer. Then the AdaIN block uses
174 "adaptive instance normalization" to transfer the style. The input images pass through a convolu-
175 tional layer containing 3×3 filters. The number of channels is increased to 32 without changing
176 the feature size, which facilitates subsequent convolution and pooling operations. Each of the four
177 downsampling blocks consists of a max-pooling layer, a dense block and two convolutional layers.
178 Among these, two convolutional layers with 1×1 filters are used to change the feature dimension.
179 The max-pooling layer implements downsampling operations to halve the feature size. Thus, with
180 each pass through a downsampling block, the width and height of the feature map becomes half
181 of the original size and the number of channels is doubled. In this way, we can obtain multi-scale
182 image information and enhance the model's ability to process high-resolution images.

183 The decoder mirrors the encoder structure, which is composed of 4 upsampling blocks to form a
184 U-Net structure. The upsampling block consists of an upsampling layer, three convolutional layers
185 and a concatenation module that receives the information coming from the "transfer module".
186 The concatenation module combines the upsampled feature and the corresponding encoder feature
187 received from the "transfer module". Using the convolutional layer to restore the required number
188 of channels, we enhance the multiplexing of features and recover more details of the input image.

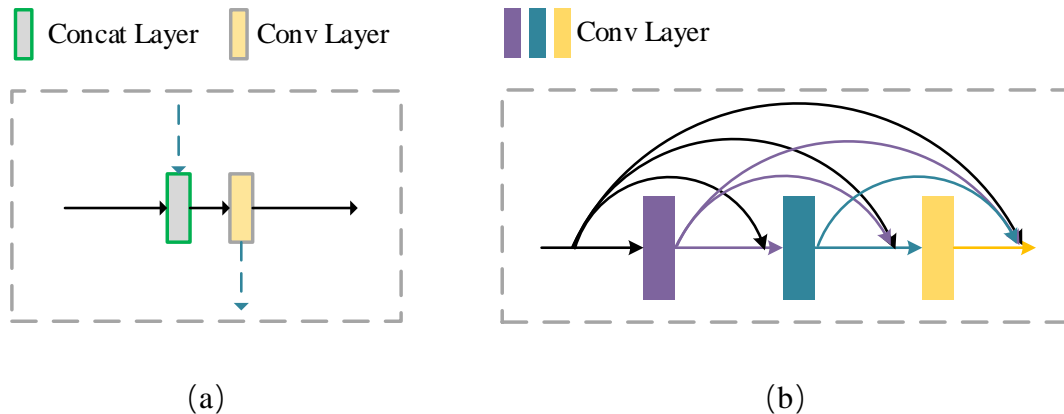


Fig 2 (a)The framework of multi-layer feature aggregation (MFA);(b)The framework of Dense Block.

189 After extracting multi-scale features, the "transfer module" is used to process the features of
 190 the content and style images with the aim of style transfer. We introduce a feature aggregation
 191 mechanism²⁶ in the "transfer module" to connect the multi-scale features of each layer. Feature
 192 aggregation enables the network to integrate spatial information from different scales and retain
 193 image detail. In order to keep more detailed information in each layer, we propose a multi-feature
 194 aggregation (MFA). As shown in Fig. 2, we insert the features of the previous to the next layer,
 195 and repeat the same feature aggregation process at the subsequent layers. Then the AdaIN method
 196 is used to stylize these aggregated features in each layer.

197 3.2 Trainig Phase

198 In the training phase, we train the network end-to-end to learn a photorealistic style transfer model.
 199 The network framework is shown in Fig. 3. In order to better extract and use image features,
 200 we use a pre-trained VGG-16 network. The trapezoids of different colors in the loss network
 201 represent different blocks. Here we use the features extracted from the first four blocks. The
 202 $relu_i_j$ indicates the output in loss network, that i indicates which block it is in VGG and j
 203 indicates which layer is in the block.

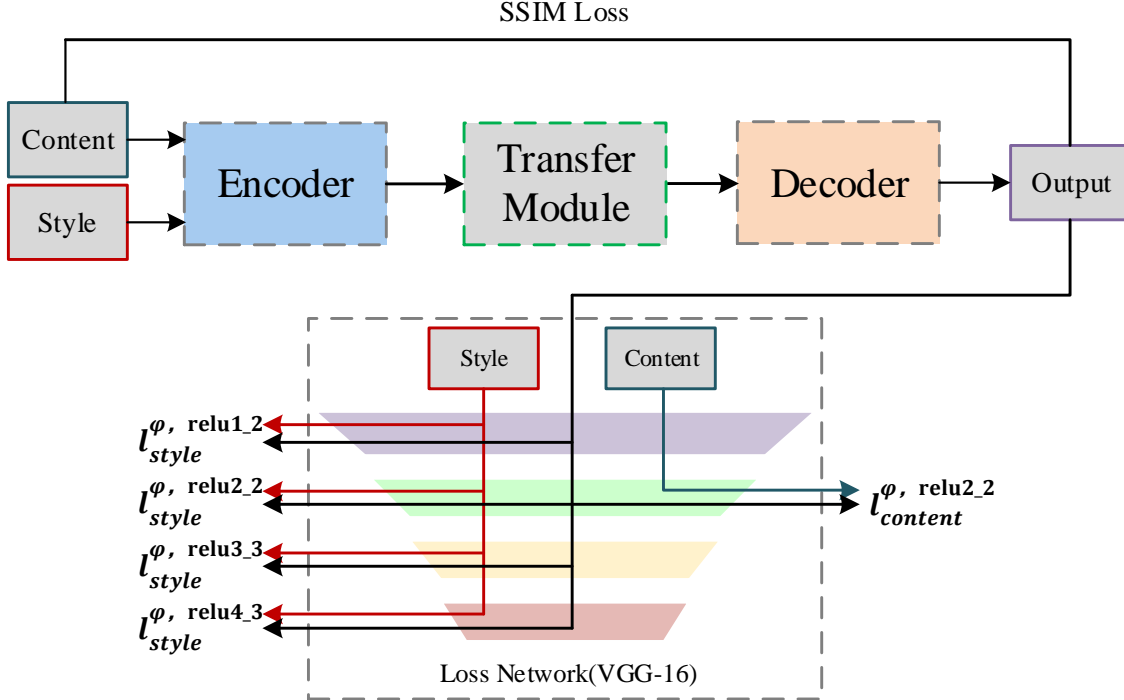


Fig 3 The framework of the training process of UMFA.

204 In the training phase, the loss function L_{total} given in Eq.1 is defined as

$$L_{total} = \alpha L_{style} + \beta L_{content} + \gamma L_{SSIM} \quad (1)$$

205 where $L_{content}$ and L_{SSIM} respectively are content loss and structure similarity(SSIM) loss be-
 206 tween the content image and output image. L_{style} is style loss between the style image and the
 207 output image. $L_{content}$ and L_{style} relate to the perceptual loss.³¹ α , β and γ are the weights of
 208 the above three losses. O , C and S represent the output image, content image and style image,
 209 respectively.

210 $l_{content}^{\varphi,j}$ is defined as the L2 norm squared of the feature which is extracted by ReLU layer in
 211 the loss network φ :

$$l_{content}^{\varphi,j}(O, C) = \frac{1}{C_j H_j W_j} \|\varphi_j(O) - \varphi_j(C)\|_2^2 \quad (2)$$

212

$$L_{content}(O, C) = l_{content}^{\varphi, relu2-2}(O, C) \quad (3)$$

213 Different from the perceptual loss, we choose the *relu2-2* as the feature layer for the content loss.

214 On the basis of the former, Gram matrix of the feature is used to represent the style feature.

215 $l_{style}^{\varphi, j}$ is calculated by Eq. 4

$$l_{style}^{\varphi, j}(O, S) = \frac{1}{C_j H_j W_j} \|G(\varphi_j(O)) - G(\varphi_j(S))\|_2^2 \quad (4)$$

$$L_{style}(O, S) = \sum_j^{relu1-2 \dots relu4-3} l_{style}^{\varphi, j}(O, S) \quad (5)$$

216 where $G(\cdot)$ denotes the calculation of Gram matrix. C , H and W are the number of channels, height

217 and width of the j -th feature map(64*256*256, 128*128*128, 256*64*64, 512*32*32). Finally,

218 the style loss L_{style} is the sum of all outputs from the four ReLU layers.

219 The SSIM loss L_{SSIM} is calculated by Eq. 6

$$L_{SSIM} = 1 - SSIM(O, C) \quad (6)$$

220 where $SSIM(\cdot)$ represents a structure similarity measure.⁴⁵ Small values of L_{SSIM} and $L_{content}$

221 means the output image O and the content image C are similar. A small value of L_{style} signifies

222 that the output image and the style image are similar.

223 4 EXPERIMENTAL RESULTS AND ANALYSIS

224 In this section, we introduce the experimental settings used during the testing phase. Then we re-
225 port the results of an ablation study. Finally, we present a subjective evaluation and some objective
226 evaluation indicators to compare the proposed method with the state of the art.

227 4.1 Experimental Setting

228 For photorealistic style transfer, any two photos can be used as style and content images. In the
229 training, we randomly divide the 80,000 pictures from MS-COCO⁴⁶ into two equal parts as the data
230 set, one part is the style image, the other part is the content image. The training process includes
231 two epochs. The training image size is set to 256×256 pixels. The Adam optimizer is used for
232 training. The learning rate is 0.0001 and unchanged. Our model is implemented with NVIDIA
233 TITAN Xp and Pytorch.

234 In the test, we use the image pairs provided in² as data set. And we verified it on other more test
235 sets.²⁰ Each set includes content, style. No masking or post-processing is used in the evaluation in
236 order to verify the effectiveness of the methods.

237 We choose three typical methods for comparison, including: "adaptive instance normalization"
238 (AdaIN),²⁷ "photorealistic image stylization based on the whitening and coloring transform" (Pho-
239 toWCT)²⁵ and "photorealistic style transfer via wavelet transforms" (WCT²).²⁰ The results are
240 obtained using publicly available codes for these methods and compared with UMFA on the same
241 benchmark.

242 Two evaluation criteria are used to quantitatively compare UMFA with other methods: struc-
243 tural similarity (SSIM) and Gram loss. Structural similarity (SSIM) measures the similarity of
244 the stylized image with the content image. The Gram loss is the mean square error between the



Fig 4 The photorealistic stylization empowered by feature aggregation. (input pair (top: content, bottom: style))

245 stylized image Gram matrix and the style image Gram matrix that represents the similarity of the
 246 style. Larger SSIM and smaller Gram loss mean better performance.

247 4.2 Ablation Study

248 **1) Feature aggregation strategy:** Feature aggregation can enrich the details of stylized images. In-
 249 spired by the bottom feature aggregation method (BFA),²⁶ we propose a multi-layer feature aggre-
 250 gation (MFA). In order to verify the effectiveness of the multi-layer feature aggregation structure,
 251 we experiment with three models: no aggregation, BFA and MFA. At this time, other parameters
 252 are set as follows: $\alpha=0.8$, $\beta:\gamma$ is 1:1 ($\beta=1$, $\gamma=1$). In Fig. 4, we show a set of images to compare the
 253 results obtained with different aggregation strategy. The plots of the total loss and style loss are
 254 shown in the Fig. 8. The results of the three aggregation strategies are summarized in Table 1.

255 As shown in Fig. 4. BFA and MFA method have similar performance, and their effect is better
 256 than inapplicable feature aggregation. The color of the sky in the red frame is closer to the style
 257 image. In Fig. 5, the convergence curves of the three methods are very close, so we operate on the
 258 values (the reciprocal of the negative logarithm). We can find that the blue line(MFA) fluctuates
 259 less during convergence which means that its convergence process is more stable. In Table 1, the
 260 results of the three methods have similar SSIM, but the result of the MFA method has a smaller
 261 Gram loss which means the results of MFA method are closer to the style of the targets. Therefore,

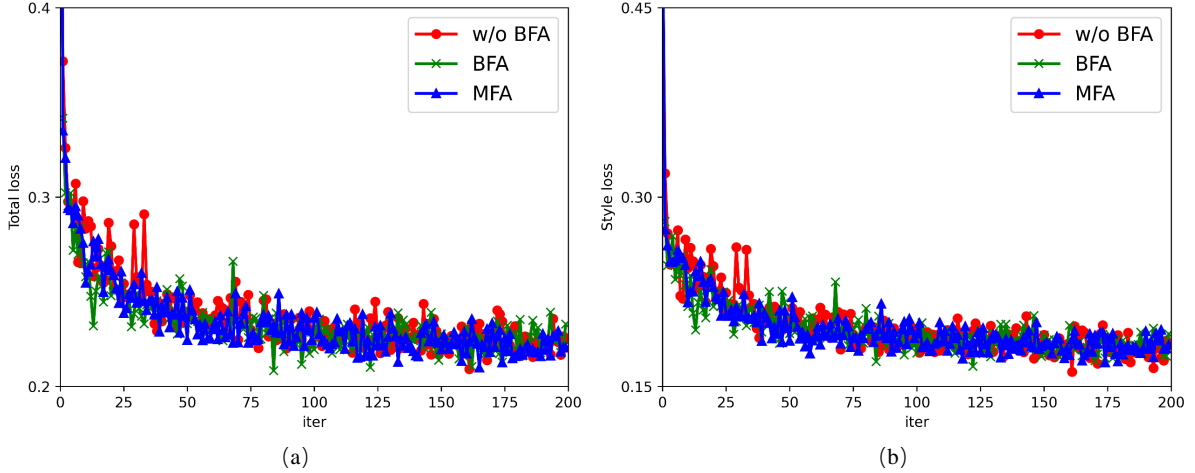


Fig 5 A plot of the evolution of the total loss(a) and style loss(b) during training (feature aggregation strategy). Each scale on the abscissa represents 100 iterations.

Table 1 The quantitative evaluation results achieved by different feature aggregation strategies

	w/o BFA	BFA	MFA
Gram loss	9.476	9.486	8.996
SSIM	0.620	0.625	0.612

262 the MFA method is used as a feature aggregation strategy.

263 **2) Parameter(α) in Loss Function:** The parameter α controls the weight of the style loss. It
 264 is set to 0.2, 0.5, 0.8. Other parameters are set as follows: $\beta:\gamma$ is 1:1 ($\beta=1, \gamma=1$), MFA is feature
 265 aggregation strategy. In Fig. 6, we show a set of images to compare the results obtained with
 266 different values of parameter α . The plots of the total loss and style loss are shown in the Fig. 7.
 267 The results of the two quantitative evaluation criteria are summarized in Table 2.

268 Fig. 6 shows the results obtained with different values of parameter α . As α increases, the
 269 degree of stylization increases visibly. The details in the red box are completely preserved, and its
 270 style is changed. In Fig. 7, the network quickly converges no matter what value the parameter α
 271 takes at 200 iterations. As the parameters α increases, the speed of the network convergence also
 272 increases. The final total loss converges to a close level. As for the style loss, the initial value is
 273 quite different for different values of parameter α . But with fast convergence, the style loss values

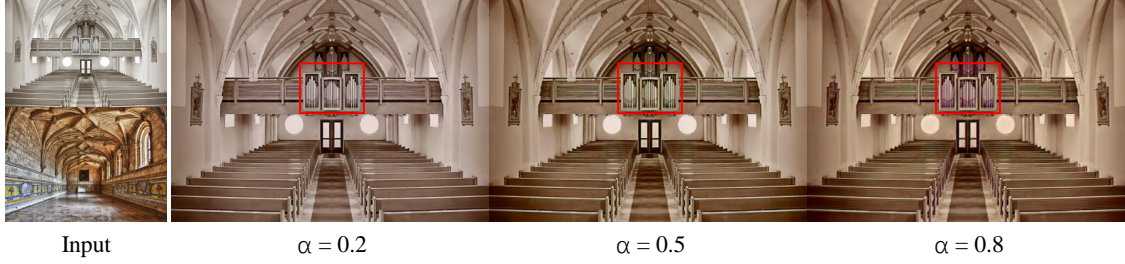


Fig 6 The photorealistic stylization results with different parameter α . (input pair (top: content, bottom: style))

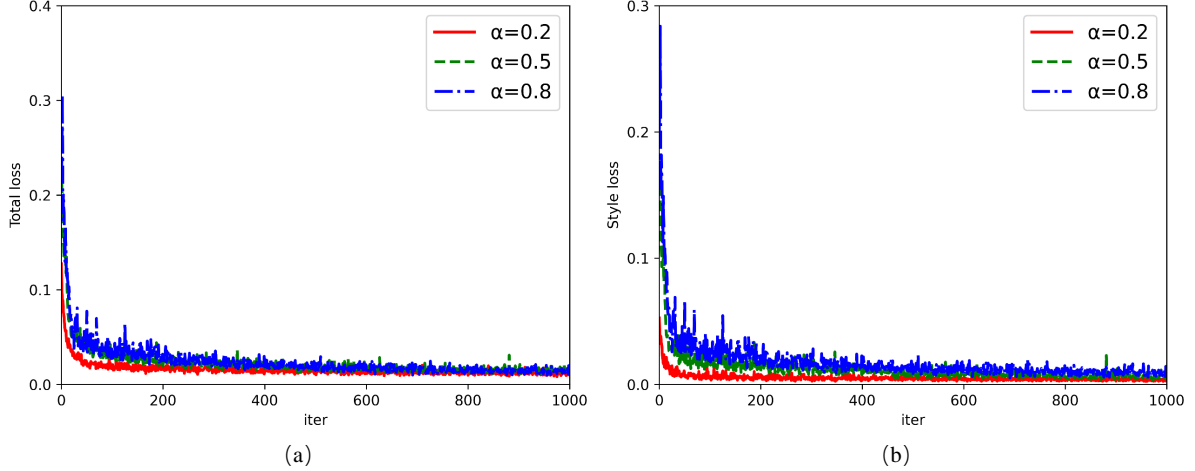


Fig 7 The evolution of the total loss(a) and style loss(b) during training (parameter α).

Table 2 Quantitative evaluation of the impact of different parameter α

	0.2	0.5	0.8
Gram loss	14.308	11.938	8.996
SSIM	0.8056	0.663	0.612

274 of becoming similar, regardless of the value of α . This shows that no matter what the value of α
 275 is, our model is stable and convergent. In the test, the largest initial value shows the smallest loss
 276 of style. This shows that we can control the stylization of the generated image by adjusting the
 277 parameters α . Since the content and style information are antagonistic, content information will be
 278 affected more when the weight of style loss is greater. As shown in Table 2, when α is large, the
 279 style evaluation is excellent but the content index is poor. Based on these observations, the value
 280 of α is set to 0.8.

281 **3) Parameters ($\beta:\gamma$) of the Loss Function:** In the,⁴⁴ Li et al. control the performance of



Fig 8 The photorealistic stylization results for different parameter values $\beta:\gamma$. (input pair (top: content, bottom: style))

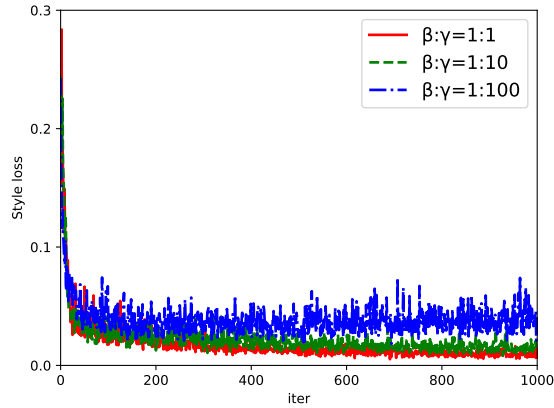


Fig 9 The evolution of the style loss during training (parameter $\beta:\gamma$).

Table 3 The impact of meta parameter $\beta:\gamma$

	1:1	1:10	1:100
Gram loss	8.996	12.726	13.922
SSIM	0.612	0.705	0.748

282 image fusion by the ratio of SSIM loss and content loss. We adopt the same strategy in our work.
 283 Accordingly, this parameter is set to 1:1, 1:10 and 1:100 ($\beta=1, \gamma=1, 10, 100$). Other parameters
 284 are set as follows: $\alpha=0.8$, MFA is used for feature aggregation. Since the change of this parameter
 285 will affect the value of the total loss, we only observe the change of style loss. Fig. 8 shows the
 286 results obtained for different values of parameter $\beta:\gamma$. The plot of style loss is shown in the Fig. 9.
 287 Table 3 summarises the results measured using the two quantitative evaluation criteria.

288 As shown in Fig. 8, the clouds in the red frame gradually become clear because of the increas-
 289 ing γ . In addition, the color distribution of the stylized image is closer to the content image, but it

290 still retains some style features, such as red mountains. This proves that the change of parameter
291 $\beta:\gamma$ can enhance the details of the content while retaining the style elements. In Fig. 9, the style
292 loss drops rapidly by the first 200 iterations. When $\beta:\gamma$ is set to 1:1, the convergence of the style
293 loss is the fastest. In addition, the blue line ($\beta:\gamma=1:100$) always exhibits large fluctuations, which
294 are difficult to stabilize. The other two lines basically converge to the same level when the param-
295 eter $\beta:\gamma$ is set as 1:1 and 1:10. As shown in Table 3, we can refine the image content by changing
296 $\beta:\gamma$, but it will lead to a loss of style. Based on these results, we choose $\beta:\gamma=1:1$ ($\beta=1, \gamma=1$).

297 4.3 Result Analysis

298 4.3.1 Subjective evaluation

299 In Fig. 10, we show the results obtained by existing methods and UMFA. The results suggest
300 that the AdaIN²⁷ method renders the highest degree of abstraction. PhotoWCT²⁵ and WCT^{2,20}
301 improved by whitening and coloring transforms (WCT), retain the structural information of the
302 image better. However, the stylization effect of these two methods is unnatural. Besides, there are
303 too many style elements that affect the realism of the photo. UMFA produces a natural stylization
304 effect, closest to a real photo with minimum artifacts.

305 In order to better verify the effect of our method on the subjective experience of people, we also
306 set up a comparison of stylized results produced by different methods. We scramble the pictures
307 generated by different methods in Fig. 10, and ask 100 testers to choose the pictures that they think
308 have the best photorealistic style transfer effect. As shown in Table 4, the percentage indicates the
309 proportion of the tester choosing the result of this method as the "Best stylization". Since they can
310 only choose one method, the sum of the overall proportions is one. Among them, the proportion
311 of choosing our method(UMFA) is the highest, that the result of UMFA is the most popular.

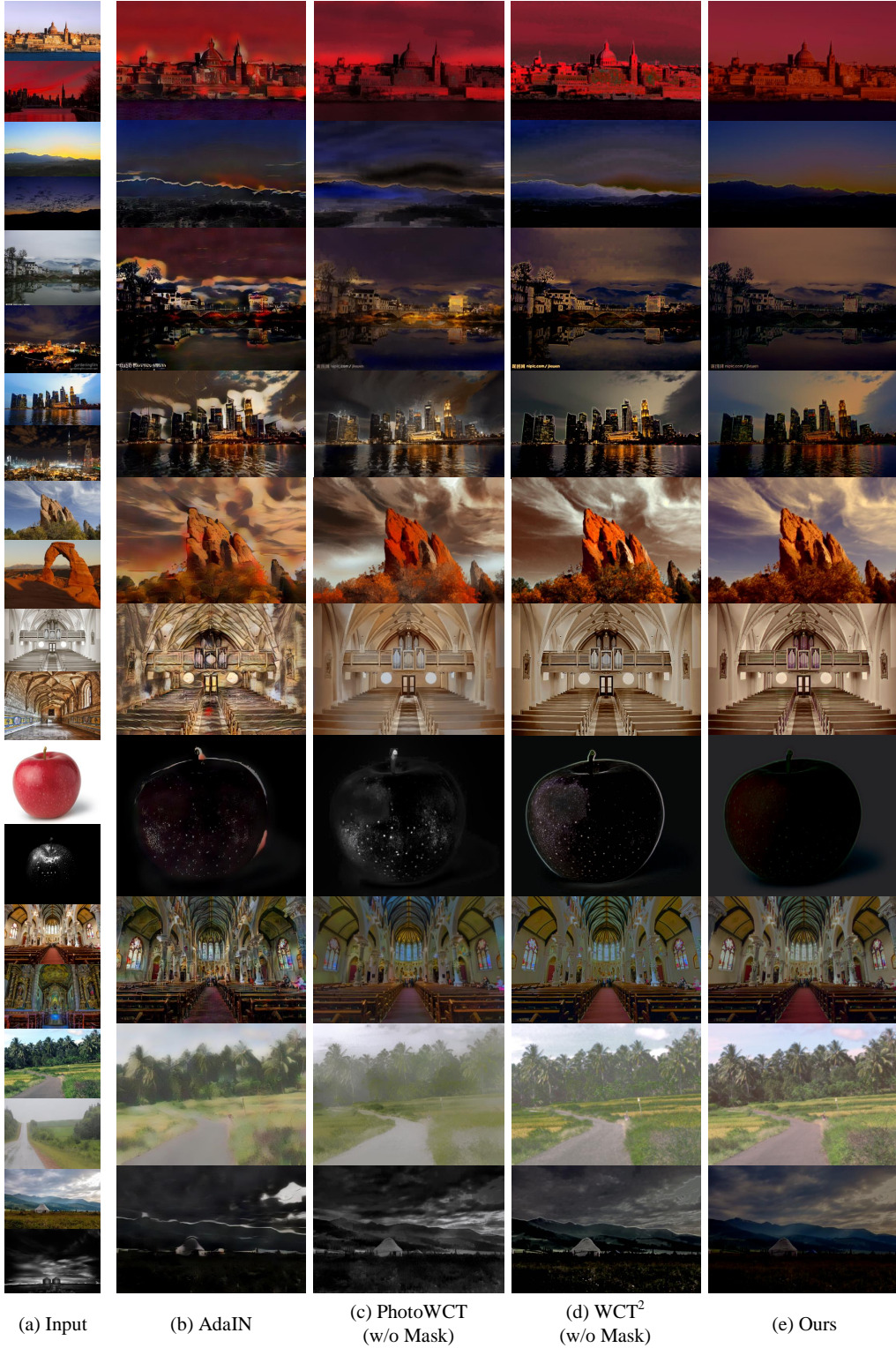


Fig 10 Photorealistic stylization results: (a) input pair (top: content, bottom: style); (b) AdaIN; (c) PhotoWCT (without mask); (d) WCT² (without mask); (e) Our method (UMFA).

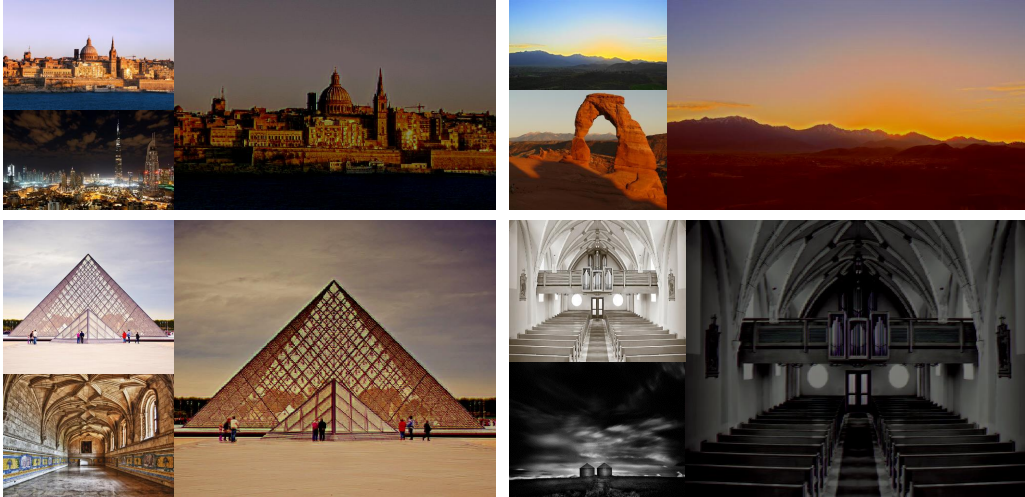


Fig 11 The result of using different structured content and style images.

Table 4 Subjective evaluation results of different methods

	AdaIN	PhotoWCT (w/o Mask)	WCT ² (w/o Mask)	Ours(UMFA)
Best stylization	13.2%	25.1%	24.8%	36.9%

312 The main purpose of photorealistic style transfer is to change the style elements of the image
 313 without changing the main body of the image content. Therefore, in order to achieve a better
 314 stylization effect, users usually use pictures with similar structures when using algorithms. In
 315 addition to the similar image structure, we also performed photorealistic style transfer tests on other
 316 images to prove the effectiveness of our method. In Fig. 11, we show four sets of photorealistic
 317 stylized images, where the upper left corner of each part is the content image, the lower left corner
 318 is the style image, and the right side is the stylized image.

319 4.3.2 Objective evaluation

320 Table 5 presents the average values of the two objective criteria used for the evaluation of stylized
 321 images (Gram loss and SSIM). The best values are indicated in **bold**. As shown in Table 5, UMFA
 322 has the smallest Gram loss and the largest SSIM which means that our photorealistic stylization

323 result has a similar style to the style image and retains the structural information of the content
324 image.

Table 5 Quantitative evaluation results of different methods

	AdaIN	PhotoWCT (w/o Mask)	WCT ² (w/o Mask)	Ours(UMFA)
Gram loss	11.356	11.367	9.323	8.996
SSIM	0.347	0.423	0.516	0.612

325 4.4 Runtime

326 Table 6 shows the runtime of AdaIN,²⁷ PhotoWCT,²⁵ WCT²²⁰ and our method(UMFA). The num-
327 bers in the table represent the time required for various methods to generate a stylized picture
328 at different image sizes. The unit of the number is seconds. The smallest values are indicated
329 in **bold** which means fastest running speed. The results of our method are denoted in **red**. For
330 PhotoWCT and WCT², we do not use mask to compare various methods at the same level. The
331 post-processing time of the PhotoWCT method is too long. We use the time of stylization process
332 as the comparison objective. AdaIn is the fastest method because it is stylized by matching the
333 mean and variance requiring the small amount of calculation. In addition, it only uses the deep-
334 est features for style transfer, reducing the amount of calculation. But for the same reason, the
335 stylization effect of the AdaIN method is the worst. PhotoWCT and WCT² take a similar amount
336 of time because they are based on the same method, but PhotoWCT needs more processing time
337 to achieve the effect closed to WCT². Compared with the Adain, the method based on whitening
338 and coloring transform requires a larger amount of calculation. Other operations introduced in the
339 encoder and decoder process further increase the runtime. Among the four methods, UMFA does
340 not take the least time. However, it can achieve real-time photorealistic style transfer and is an

341 order of magnitude faster than the other two popular methods. Inspired by AdaIN, we changed the
 342 network structure, added MFA blocks and perform multi-layer stylization operations. As a result,
 we have achieved a balance between photorealistic stylization and time consumption.

Table 6 A comparison of runtime for different methods(Time/sec)

Image Size	AdaIN	PhotoWCT	WCT ²	Ours(UMFA)
256 × 256	0.046	3.44	5.04	0.14
512 × 512	0.12	3.48	5.64	0.24
1024 × 1024	0.35	3.66	6.06	0.64

343

344 5 CONCLUSION

345 In this paper, we propose a photorealistic style transfer model named UMFA based on U-Net and
 346 multi-layer feature aggregation. First, the encoder, which uses the dense block in the downsam-
 347 pling module, can make full use of the image information to capture details. The "transfer module"
 348 is designed to enrich multi-scale features and enhance the expressiveness of stylization results by
 349 AdaIN and MFA blocks. The upsampling and skip connection of the U-Net structure are designed
 350 for the decoder to reconstruct and output the stylized image. The experimental results show that
 351 the UMFA method enhances the content detail in the stylized image and retains the texture of the
 352 photo, achieving style transfer with a natural photorealistic effect.

353 6 Acknowledgments

354 This work was supported by the National Key Research and Development Program of China
 355 (Grant No. 2017YFC1601800), the National Natural Science Foundation of China (61672265,
 356 U1836218), the 111 Project of Ministry of Education of China (B12018), and the UK EPSRC
 357 (EP/N007743/1, MURI/EPSRC/DSTL, EP/R018456/1).

358 *References*

- 359 1 P.-Y. Laffont, Z. Ren, X. Tao, *et al.*, “Transient attributes for high-level understanding and
360 editing of outdoor scenes,” *ACM Transactions on graphics (TOG)* **33**(4), 1–11 (2014).
- 361 2 F. Luan, S. Paris, E. Shechtman, *et al.*, “Deep photo style transfer,” in *Proceedings of the*
362 *IEEE Conference on Computer Vision and Pattern Recognition*, 4990–4998 (2017).
- 363 3 A. Akl, C. Yaacoub, M. Donias, *et al.*, “A survey of exemplar-based texture synthesis meth-
364 ods,” *Computer Vision and Image Understanding* **172**, 12–24 (2018).
- 365 4 A. A. Efros and W. T. Freeman, “Image quilting for texture synthesis and transfer,” in *Pro-*
366 *ceedings of the 28th annual conference on Computer graphics and interactive techniques*,
367 341–346 (2001).
- 368 5 Z.-C. Song and S.-G. Liu, “Sufficient image appearance transfer combining color and tex-
369 ture,” *IEEE Transactions on Multimedia* **19**(4), 702–711 (2016).
- 370 6 L. A. Gatys, A. S. Ecker, and M. Bethge, “Image style transfer using convolutional neural net-
371 works,” in *Proceedings of the IEEE conference on computer vision and pattern recognition*,
372 2414–2423 (2016).
- 373 7 X. Zhang, Y. Luan, and X. Li, “Real-time image style transformation based on deep learning,”
374 *Journal of Electronic Imaging* **27**(4), 043045 (2018).
- 375 8 H. Zhang and K. Dana, “Multi-style generative network for real-time transfer,” in *Proceed-*
376 *ings of the European Conference on Computer Vision (ECCV)*, 0–0 (2018).
- 377 9 A. Krizhevsky, I. Sutskever, and G. E. Hinton, “Imagenet classification with deep convolu-
378 tional neural networks,” in *Advances in neural information processing systems*, 1097–1105
379 (2012).

- 380 10 Y. Jing, Y. Yang, Z. Feng, *et al.*, “Neural style transfer: A review,” *IEEE transactions on*
381 *visualization and computer graphics* (2019).
- 382 11 L. A. Gatys, A. S. Ecker, M. Bethge, *et al.*, “Controlling perceptual factors in neural style
383 transfer,” in *Proceedings of the IEEE Conference on Computer Vision and Pattern Recognition*,
384 3985–3993 (2017).
- 385 12 S. Gu, C. Chen, J. Liao, *et al.*, “Arbitrary style transfer with deep feature reshuffle,” in *Pro-*
386 *ceedings of the IEEE Conference on Computer Vision and Pattern Recognition*, 8222–8231
387 (2018).
- 388 13 M.-M. Cheng, X.-C. Liu, J. Wang, *et al.*, “Structure-preserving neural style transfer,” *IEEE*
389 *Transactions on Image Processing* **29**, 909–920 (2019).
- 390 14 Z. Hu, J. Jia, B. Liu, *et al.*, “Aesthetic-aware image style transfer,” in *Proceedings of the 28th*
391 *ACM International Conference on Multimedia*, 3320–3329 (2020).
- 392 15 O. Texler, D. Futschik, J. Fišer, *et al.*, “Arbitrary style transfer using neurally-guided patch-
393 based synthesis,” *Computers & Graphics* **87**, 62–71 (2020).
- 394 16 M. Li, C. Ye, and W. Li, “High-resolution network for photorealistic style transfer,” *arXiv*
395 *preprint arXiv:1904.11617* (2019).
- 396 17 S. Yang, W. Wang, and J. Liu, “Te141k: Artistic text benchmark for text effect transfer,”
397 *IEEE Transactions on Pattern Analysis and Machine Intelligence* (2020).
- 398 18 G. Li, J. Zhang, D. Chen, *et al.*, “Chinese flower-bird character generation based on pencil
399 drawings or brush drawings,” *Journal of Electronic Imaging* **28**(3), 033029 (2019).
- 400 19 L. Wang, Z. Wang, X. Yang, *et al.*, “Photographic style transfer,” *The Visual Computer* **36**(2),
401 317–331 (2020).

- 402 20 J. Yoo, Y. Uh, S. Chun, *et al.*, “Photorealistic style transfer via wavelet transforms,” in *Pro-*
403 *ceedings of the IEEE International Conference on Computer Vision*, 9036–9045 (2019).
- 404 21 K. Sunkavalli, M. K. Johnson, W. Matusik, *et al.*, “Multi-scale image harmonization,” *ACM*
405 *Transactions on Graphics (TOG)* **29**(4), 1–10 (2010).
- 406 22 F. Pitie, A. C. Kokaram, and R. Dahyot, “N-dimensional probability density function transfer
407 and its application to color transfer,” in *Tenth IEEE International Conference on Computer*
408 *Vision (ICCV’05) Volume 1*, **2**, 1434–1439, IEEE (2005).
- 409 23 J.-D. Yoo, M.-K. Park, J.-H. Cho, *et al.*, “Local color transfer between images using dominant
410 colors,” *Journal of Electronic Imaging* **22**(3), 033003 (2013).
- 411 24 A. Levin, D. Lischinski, and Y. Weiss, “A closed-form solution to natural image matting,”
412 *IEEE transactions on pattern analysis and machine intelligence* **30**(2), 228–242 (2007).
- 413 25 Y. Li, M.-Y. Liu, X. Li, *et al.*, “A closed-form solution to photorealistic image stylization,” in
414 *Proceedings of the European Conference on Computer Vision (ECCV)*, 453–468 (2018).
- 415 26 J. An, H. Xiong, J. Huan, *et al.*, “Ultrafast photorealistic style transfer via neural architecture
416 search.,” in *AAAI*, 10443–10450 (2020).
- 417 27 X. Huang and S. Belongie, “Arbitrary style transfer in real-time with adaptive instance nor-
418 malization,” in *Proceedings of the IEEE International Conference on Computer Vision*, 1501–
419 1510 (2017).
- 420 28 O. Ronneberger, P. Fischer, and T. Brox, “U-net: Convolutional networks for biomedical im-
421 age segmentation,” in *International Conference on Medical image computing and computer-*
422 *assisted intervention*, 234–241, Springer (2015).

- 423 29 F. Yu, D. Wang, E. Shelhamer, *et al.*, “Deep layer aggregation,” in *Proceedings of the IEEE*
424 *conference on computer vision and pattern recognition*, 2403–2412 (2018).
- 425 30 K. Simonyan and A. Zisserman, “Very deep convolutional networks for large-scale image
426 recognition,” in *International Conference on Learning Representations*, (2015).
- 427 31 J. Johnson, A. Alahi, and L. Fei-Fei, “Perceptual losses for real-time style transfer and super-
428 resolution,” in *European conference on computer vision*, 694–711, Springer (2016).
- 429 32 V. Dumoulin, J. Shlens, and M. Kudlur, “A learned representation for artistic style,” *arXiv*
430 *preprint arXiv:1610.07629* (2016).
- 431 33 D. Ulyanov, A. Vedaldi, and V. Lempitsky, “Improved texture networks: Maximizing quality
432 and diversity in feed-forward stylization and texture synthesis,” in *Proceedings of the IEEE*
433 *Conference on Computer Vision and Pattern Recognition*, 6924–6932 (2017).
- 434 34 Y. Li, C. Fang, J. Yang, *et al.*, “Universal style transfer via feature transforms,” in *Advances*
435 *in neural information processing systems*, 386–396 (2017).
- 436 35 B. Zoph and Q. Le, “Neural architecture search with reinforcement learning,” in *International*
437 *Conference on Learning Representations*, (2017).
- 438 36 P. Isola, J.-Y. Zhu, T. Zhou, *et al.*, “Image-to-image translation with conditional adversarial
439 networks,” in *Proceedings of the IEEE conference on computer vision and pattern recogni-*
440 *tion*, 1125–1134 (2017).
- 441 37 B. Cao, H. Zhang, N. Wang, *et al.*, “Auto-gan: self-supervised collaborative learning for
442 medical image synthesis,” in *Proceedings of the AAAI Conference on Artificial Intelligence*,
443 **34**(07), 10486–10493 (2020).

- 444 38 Y.-F. Zhou, R.-H. Jiang, X. Wu, *et al.*, “Branchgan: Unsupervised mutual image-to-image
445 transfer with a single encoder and dual decoders,” *IEEE Transactions on Multimedia* **21**(12),
446 3136–3149 (2019).
- 447 39 J.-Y. Zhu, T. Park, P. Isola, *et al.*, “Unpaired image-to-image translation using cycle-
448 consistent adversarial networks,” in *Proceedings of the IEEE international conference on*
449 *computer vision*, 2223–2232 (2017).
- 450 40 D. Liu, B. Wen, X. Liu, *et al.*, “When image denoising meets high-level vision tasks: A deep
451 learning approach,” *arXiv preprint arXiv:1706.04284* (2017).
- 452 41 K. He, X. Zhang, S. Ren, *et al.*, “Identity mappings in deep residual networks,” in *European*
453 *conference on computer vision*, 630–645, Springer (2016).
- 454 42 K. He, X. Zhang, S. Ren, *et al.*, “Deep residual learning for image recognition,” in *Proceed-*
455 *ings of the IEEE conference on computer vision and pattern recognition*, 770–778 (2016).
- 456 43 G. Huang, Z. Liu, L. Van Der Maaten, *et al.*, “Densely connected convolutional networks,” in
457 *Proceedings of the IEEE conference on computer vision and pattern recognition*, 4700–4708
458 (2017).
- 459 44 H. Li and X.-J. Wu, “Densefuse: A fusion approach to infrared and visible images,” *IEEE*
460 *Transactions on Image Processing* **28**(5), 2614–2623 (2018).
- 461 45 Z. Wang, A. C. Bovik, H. R. Sheikh, *et al.*, “Image quality assessment: from error visibility
462 to structural similarity,” *IEEE transactions on image processing* **13**(4), 600–612 (2004).
- 463 46 T.-Y. Lin, M. Maire, S. Belongie, *et al.*, “Microsoft coco: Common objects in context,” in
464 *European conference on computer vision*, 740–755, Springer (2014).

465 **Dongyu Rao** received the B.E. degree in School of Metallurgy and Environment from Central
466 South University, China, in 2019. He is a master student at the Jiangsu Provincial Engineering
467 Laboratory of Pattern Recognition and Computational Intelligence, School of Artificial Intelli-
468 gence and Computer Science, Jiangnan University. His research interests include style transfer,
469 machine learning and deep learning.

470 **Xiao-Jun Wu** received the Ph.D. degree in pattern recognition and intelligent system from the
471 Nanjing University of Science and Technology, Nanjing, in 2002. He has been with the School of
472 Information Engineering, Jiangnan University since 2006, where he is a Professor of pattern recog-
473 nition and computational intelligence. He has published over 300 papers in his fields of research.
474 His current research interests include pattern recognition, computer vision, and computational in-
475 telligence.

476 **Hui Li** received the B.Sc. degree in School of Internet of Things Engineering from Jiangnan
477 University, China, in 2015. He is currently a PhD student at the Jiangsu Provincial Engineering
478 Laboratory of Pattern Recognition and Computational Intelligence, School of Artificial Intelli-
479 gence and Computer Science, Jiangnan University. His research interests include image fusion,
480 machine learning and deep learning.

481 **Josef Kittler** received the B.A., Ph.D., and D.Sc. degrees from the University of Cambridge, in
482 1971, 1974, and 1991, respectively. He is a distinguished Professor of Machine Intelligence at the
483 Centre for Vision, Speech and Signal Processing, University of Surrey, U.K. He conducts research
484 in biometrics, video and image database retrieval, medical image analysis, and cognitive vision.
485 He published the textbook Pattern Recognition: A Statistical Approach and over 700 scientific

486 papers.

487 **Tianyang Xu** received the B.Sc. degree in electronic science and engineering from Nanjing Uni-
488 versity, Nanjing, China, in 2011. He received the PhD degree at the School of Internet of Things
489 Engineering, Jiangnan University, Wuxi, China, in 2019. He is currently a research fellow at the
490 Centre for Vision, Speech and Signal Processing (CVSSP), University of Surrey, Guildford, United
491 Kingdom. His research interests include visual tracking and deep learning.

492 **List of Figures**

493	1	The framework of our method.	8
494	2	(a)The framework of multi-layer feature aggregation (MFA);(b)The framework of	
495		Dense Block.	10
496	3	The framework of the training process of UMFA.	11
497	4	The photorealistic stylization empowered by feature aggregation. (input pair (top:	
498		content, bottom: style))	14
499	5	A plot of the evolution of the total loss(a) and style loss(b) during training (feature	
500		aggregation strategy). Each scale on the abscissa represents 100 iterations.	15
501	6	The photorealistic stylization results with different parameter α . (input pair (top:	
502		content, bottom: style))	16
503	7	The evolution of the total loss(a) and style loss(b) during training (parameter α).	16
504	8	The photorealistic stylization results for different parameter values $\beta:\gamma$. (input pair	
505		(top: content, bottom: style))	17
506	9	The evolution of the style loss during training (parameter $\beta:\gamma$).	17

507	10	Photorealistic stylization results: (a) input pair (top: content, bottom: style); (b)	
508		AdaIN; (c) PhotoWCT (without mask); (d) WCT ² (without mask); (e) Our method	
509		(UMFA).	19
510	11	The result of using different structured content and style images.	20

511 **List of Tables**

512	1	The quantitative evaluation results achieved by different feature aggregation strategies	15
513	2	Quantitative evaluation of the impact of different parameter α	16
514	3	The impact of meta parameter $\beta:\gamma$	17
515	4	Subjective evaluation results of different methods	20
516	5	Quantitative evaluation results of different methods	21
517	6	A comparison of runtime for different methods(Time/sec)	22